Dalton Transactions

ROYAL SOCIETY OF CHEMISTRY

COMMUNICATION

View Article Online
View Journal

Cite this: DOI: 10.1039/d0dt03788e

Received 3rd November 2020,
Accepted 1st December 2020

DOI: 10.1039/d0dt03788e

rsc.li/dalton

Stepwise enhancement of fluorescence induced by anion coordination and non-covalent interactions†

Dan Zhang, ‡ Jie Zhao,‡ Liping Cao, * Dong Yang, Bozhong Chen, Le Yu, Xiao-Juan Yang and Biao Wu *

A multi-level regulation of fluorescence enhancement upon anion coordination and subsequent binding of a guest (methyl viologen) was presented by a bis–bis(urea)-decorated tetraphenylethene (TPE) ligand with an assembly-enhanced emission characteristic.

Fluorescence enhancement has attracted considerable attention owing to both easily detected sensing event and its potential applications as diagnostic, monitoring and analytical tools in medical, biochemical, and environmental science.[1] However, conventional luminophores used in the real world tend to exhibit fluorescence quenching because of their aggregation.[2] Luminogens with the feature of aggregation-induced emission (AIE),[3] especially tetraphenylethene (TPE), have been extensively studied in the past twenty years due to the brightened emission by aggregate formation and wide range of applications such as fluorescence "turn-on" or "light-up" biosensors,[4] biological/chemical probes,[5] biological imaging,[6] light-harvesting,[7] circularly polarized luminescence materials,[8] and so on. In previous research, the TPE group has been incorporated to metal–organic frameworks (MOFs),[9] covalent organic frameworks (COFs),[10] supramolecular organic frameworks (SOFs),[11] donor–acceptor (D–A) complexes,[12] porous materials,[13] polymers,[14] macrocycles,[15] and cages.[16]

In contrast to the well-studied supramolecular architectures containing transition metal ions, the anion-coordination-driven assembly (ACDA) strategy has been overlooked for a long time due to the intrinsic properties and lack of reliable coordination geometry of anions.[17] In recent years, a series of A_4L_4 and A_4L_6 (A = anion) tetrahedral anion cages and A_2L_3 triple anion helicates have been successfully achieved, demonstrating that anions could also act as coordination centers to construct diverse supramolecular architectures like metal ions.[18] The anion-coordination-driven cages and helicates possess the capacity for encapsulation of guest molecules, stabilizing active molecules and controlling reactivity.[19] Nevertheless, the exploration of the applications in more aspects, such as catalysis, drug delivery, gas absorption and storage, as well as sensing, still needs more efforts.

In order to explore ACDA and its potential applications in fluorescent materials and biosensors, we previously reported the tetrakis(bisurea)-decorated tetraphenylethene ligand, showing fluorescence "turn-on" properties upon coordination with phosphate ions in a wide range of concentrations.[20] Inspired by this work, we expect to utilize ligand **L**, in which two bis(urea) moieties are attached to a tetraphenylethene (TPE) core (Scheme 1), to achieve multi-level regulation of fluorescence enhancement by anion coordination and guest binding. According to our previous work,[21] such bis–bis(urea) ligands have the potential to form a discrete motif through coordination to phosphate anions. Interestingly, **L** assembled complexes, exhibiting obvious "turn-on" fluorescence.

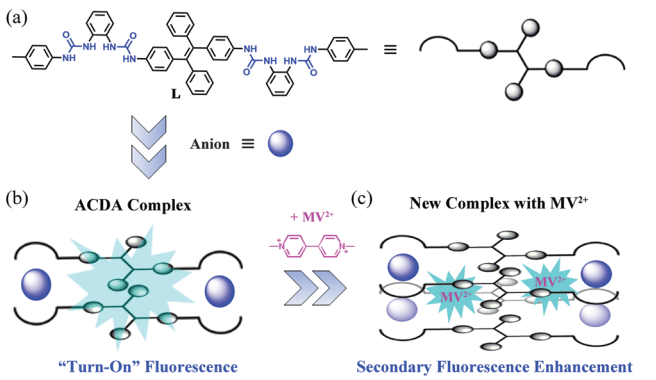

Scheme 1 (a) Chemical structure of ligand **L**; (b) first-level "turn-on" fluorescence in a TPE rotor by ACDA and aggregation; (c) second-level fluorescence enhancement by adding guest MV^{2+}.

Key Laboratory of Synthetic and Natural Functional Molecule Chemistry of the Ministry of Education, College of Chemistry and Materials Science, Northwest University, Xi'an 710127, China. E-mail: chcaoliping@nwu.edu.cn, wubiao@nwu.edu.cn

†Electronic supplementary information (ESI) available. CCDC 2025855–2025857. For ESI and crystallographic data in CIF or other electronic format see DOI: 10.1039/d0dt03788e

‡These authors contributed equally to this work.

Moreover, the fluorescence is further enhanced by introducing a guest cation (methyl viologen, MV^{2+}), which is bound by non-covalent interactions between the two anion complexes. Herein the multi-level regulation of the fluorescence of TPE is reported (Scheme 1).

The bis–bis(urea) ligand **L** was synthesized by a four-step strategy and the product (**A**) of the first step was purified from a mixture of (*Z*) and (*E*) isomers[22] (for synthetic details see the ESI†). First of all, single crystals of the monohydrogen phosphate complex, $[K([18]crown\text{-}6)]_4[(HPO_4)_2(\mathbf{L})_2]$ (**1**) (the phosphate anion was generated *in situ* from K_3PO_4 and [18]crown-6, and [18]crown-6 is used to dissolve K_3PO_4 in an organic solvent) were obtained. Complex **1** shows a 2 : 2 anion-to-ligand ratio, in which two ligands stack to embrace two anions (Fig. 1a), similar to the monohydrogen phosphate complex of the tetrakis(bisurea)-decorated TPE ligand in our previous work.[21] Four $[K([18]crown\text{-}6)]^+$ counter cations situate around complex **1** and form weak C–H···π interactions with the dangling phenyl rings of TPE (3.556–3.776 Å, Fig. S9b†), contributing to the restriction of the intramolecular rotation of TPE and fluorescence enhancement. Two of them coordinate to the O atoms of urea groups and the other two interact with the O atoms of HPO_4^{2-}. Both HPO_4^{2-} anions are coordinated by four urea groups from two bis(urea) moieties through eight N–H···O hydrogen bonds (N···O distances in the range of 2.748–2.974 Å and N–H···O angles from 144° to 162°). The ^{1}H NMR spectra showed the distinct downfield shifts of –NH signals (avg $\Delta\delta$ = 2.26 ppm) and the upfield shift of $-CH_3$ of **L** ($\Delta\delta$ = −0.11 ppm, Fig. 1c) compared with ligand **L**. ^{1}H NMR titration of **L** with HPO_4^{2-} (0–2.0 equiv., generated *in situ* from K_2HPO_4 and [18]crown-6) showed that the peaks remain unchanged after 1.0 equiv. (Fig. S12†). Combined with the solid-state structure, it appears that **L** and HPO_4^{2-} assembled in the 2 : 2 mode. The DOSY spectrum showed that complex **1** is a single assembly (Fig. S22†). The ESI-MS study confirmed the 2 : 2 stoichiometry $[\mathbf{L}_2(HPO_4)_2([18]crown\text{-}6)K]^{3-}$ (obsd 762.93 *vs.* calcd 762.93) and $[\mathbf{L}_2(HPO_4)_2([18]crown\text{-}6)_2K_2]^{2-}$ (obsd 1295.96 *vs.* calcd 1295.96) (Fig. S26†).

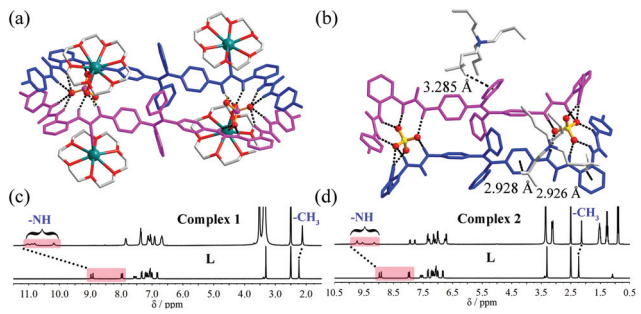

Fig. 1 (a) Crystal structure of $[(HPO_4)_2(\mathbf{L})_2]^{4-}$ (**1**) showing the coordination of two HPO_4^{2-} anions by two ligands; (b) crystal structure of $[(SO_4)_2(\mathbf{L})_2]^{4-}$ (**2**) with the coordination of two SO_4^{2-} anions by two ligands and cation–π interactions between TBA^+ and phenyl; and ^{1}H NMR spectra (400 MHz, 298 K, [D$_6$]DMSO) of complex **1** (c) and complex **2** (d).

The complex $[TBA]_4[(SO_4)_2(\mathbf{L})_2]$ (**2**) also shows a 2 : 2 structure similar to **1** despite the different counter-cation. The SO_4^{2-} anions are bound through eight N–H···O hydrogen bonds, respectively, ranging from 2.773 Å to 3.023 Å. Four TBA^+ counter-cations are located around the $[(SO_4)_2(\mathbf{L})_2]^{4-}$ moiety and two of them interact with phenyl rings of TPE cores through cation–π interactions (Fig. 1b). A comparison of the two anion complexes demonstrates that the shortest phenyl···phenyl separation between the two TPE cores within one $A_2\mathbf{L}_2$ complex is 4.105 Å (C18···C41; Fig. S6a†) for complex **1**, and 3.562 Å (C19···C38) and 3.585 Å (C64···C69; Fig. S10†) for **2**. The ^{1}H NMR spectra showed the obvious downfield shifts of –NH (avg $\Delta\delta$ = 1.08 ppm) and the upfield shift of $-CH_3$ ($\Delta\delta$ = −0.09 ppm, Fig. 1d) compared with ligand **L**. From ^{1}H NMR titration (0–2.0 equiv.), a two-step binding process was observed that changed from 1 : 1 to 1 : 2 (**L** : **A**, Fig. S13†) with more added anions. Due to there are two types of assembly in the binding of **L** with SO_4^{2-}, the details such as the binding ratio cannot be obtained. However, by comparison, it can be found that titration of the 1 : 1 mode is consistent with complex **2**. Namely, in solution, the binding of **L** with SO_4^{2-} is 2 : 2. ^{1}H NMR variable temperature and concentration experiments indicated that the coordination of **L** with anions is stable in complexes **1** and **2** as the 2 : 2 mode (Fig. S16, S17 and S19, S20†), and the DOSY spectrum revealed that complex **2** is a single assembly (Fig. S23†). The ESI-MS study confirmed its composition $[\mathbf{L}_2(SO_4)_2(TBA)]^{3-}$ (obsd 742.62 *vs.* calcd 742.62) and $[\mathbf{L}_2(SO_4)_2(TBA)_2]^{2-}$ (obsd 1235.11 *vs.* calcd 1235.11) (Fig. S27†).

Subsequently, the binding behaviors of **L** with different anions were examined by employing fluorescence experiments (Fig. 2). With the addition of 1.0 equiv. of PO_4^{3-} or HPO_4^{2-} ions, the emission intensity increased by about 14-fold and 12-fold, respectively, along with 30 nm red shifts. Adding 1.0 equiv. of SO_4^{2-} ions caused about 6-fold fluorescence enhancement, while other anions induced no obvious change (*e.g.*, NO_3^-, Br^-, Cl^-, ClO_4^-, I^-, HSO_4^-, $H_2PO_4^-$, AcO^-, and F^-, as TBA^+ salts; 1.0 equiv.).

The most interesting aspect of the assembly of **L** with phosphate may be fluorescence enhancement. However, in the solution state, the anion exists as a mixture of PO_4^{3-} and HPO_4^{2-} (^{1}H NMR titration, see Fig. S14†), and the binding depends on the concentration. As the concentration increases, the PO_4^{3-} assembly tends to form (**L** = 40 mM, Fig. S15†). The ESI-MS

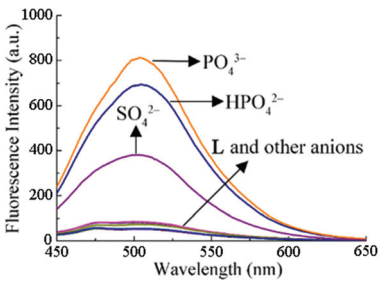

Fig. 2 Fluorescence emission spectra (λ_{ex} = 415 nm) of L (1.0 × 10^{-4} M in DMSO) upon the addition of 1.0 equiv. of different anions.

study demonstrated the formation of $[\mathbf{L}_2(PO_4)_2([18]crown\text{-}6)_4K_4]^{2-}$ (obsd 1598.07 *vs.* calcd 1598.07) and $[\mathbf{L}_2(PO_4)_1(HPO_4)_1([18]crown\text{-}6)_3K_3]^{2-}$ (obsd 1447.52 *vs.* calcd 1447.52) (Fig. S28†), the latter indicating the coexistence of two anions in the system. Unfortunately, we cannot obtain single crystals, but PM6 calculation on **L** with phosphate (2 : 2) supports the rationality of this structure (Fig. S34†). In addition, the DOSY spectrum also showed the generation of a solely 2 : 2 complex in a concentrated solution (Fig. S24†).

As we know, methyl viologen (MV^{2+}) possesses excellent electron-accepting properties and is an efficient electron-transfer medium,[23] which is likely to interact with electron-rich systems such as anion complexes **1** and **2**. Hence, it is expected that MV^{2+} can be utilized as a guest to further change the fluorescence of an anion assembly. When 2.0 equiv. of methyl viologen dichloride ($MVCl_2$, dissolved in water) was added to the solution of **L** (1.0×10^{-4} M) with 1.0 equiv. of phosphate anions (generated from K_3PO_4 and [18]crown-6) in DMSO, the fluorescence intensity further increased with a red shift ($\Delta\lambda$ = 44 nm) (Fig. 3a). The ^{1}H NMR spectra demonstrated that the assembly transformed from mixed anions to a single complex in solution after the addition of $MVCl_2$ (Fig. S25†). Notably, the addition of 2.0 equiv. of $MVCl_2$ to a solution containing only phosphate anions (1.0×10^{-4} M) also induced fluorescence emission, which may be due to the electrostatic interaction and alkaline environment.[24] In order to study the mechanism of the fluorescence enhancement, both excitation and emission spectra were collected. The emission spectrum of **L** with 1.0 equiv. of PO_4^{3-} (λ_{ex} = 415 nm), and the excitation spectra of **L** with 1.0 equiv. of PO_4^{3-} and 2.0 equiv. of $MVCl_2$ (λ_{em} = 544 nm), as well as the excitation spectra of phosphate anions (1.0×10^{-4} M) and 2.0 equiv. of $MVCl_2$ (λ_{em} = 544 nm) were obtained (Fig. 3b). From Fig. 3b we can find the partial overlap between the emission spectrum (**L** with PO_4^{3-}) and excited spectrum (**L** with PO_4^{3-} and $MVCl_2$; PO_4^{3-} with $MVCl_2$), which indicated that the second-step fluorescence enhancement may arise from MV^{2+}. Meanwhile, compared with the fluorescence of **L**, there is no change after adding $MVCl_2$, indicating that $MVCl_2$ alone has no interaction with **L** (Fig. S29†).

UV-vis studies on the binding property of **L** to phosphate anions have also been carried out in DMSO (1.0×10^{-4} M). Addition of 1.0 equiv. of phosphate anions (as the [18]crown-6-K salt) to the DMSO solution of **L** induced a bathochromic shift of the spectrum. A new intense broad absorption band at 467 nm was formed when 2.0 equiv. of $MVCl_2$ was added to the solution of **L** with 1.0 equiv. of phosphate anions (Fig. 4a), which is consistent with the optimum excitation wavelength of the phosphate complex containing MV^{2+} (complex **3**) and favours the interaction between MV^{2+} and complex **1** in the newly formed complex **3** (Fig. 3b). The UV-vis spectrum of phosphate anions (1.0×10^{-4} M) with 2.0 equiv. of $MVCl_2$ in DMSO shows a broad absorption band at 410 nm. The UV-vis titration experiments revealed the binding constants, $K_1 = 4.04 \times 10^5$ M^{-1} and $K_2 = 1.05 \times 10^4$ M^{-1} (see the ESI, Fig. S31†). Meanwhile, the fluorescence emission of complex **1** (1.0×10^{-4} M in DMSO) decreased at 500 nm along with the increase of a new emission at 544 nm upon the addition of 0–4.0 equiv. of $MVCl_2$ (Fig. 4b), which suggests that the emission wavelength has changed with the formation of the new complex **3**. It was found that complex **3** and the $MVCl_2$/phosphate system possess the same emission wavelength, which indicates that the fluorescence of TPE gradually decreased due to a photo-induced electron transfer (PET) process between the anion complex and MV^{2+}. The fluorescence enhancement at 544 nm, which belongs to MV^{2+}, is caused by electrostatic and other non-covalent interactions between the anion complex and MV^{2+}.

The interaction between the anion complex and MV^{2+} was proved by the crystal structure of the sulfate complex $[(MV)\mathbf{L}SO_4]_2$ (**4**) from the mixture of sulfate ions, ligand **L**, and MV^{2+}. Compared with complex **2**, SO_4^{2-} anions exhibit one less hydrogen bond in complex **4**. Only seven N–H···O hydrogen bonds were formed (N···O distances in the range of 2.79–3.03 Å, and N–H···O angles from 145° and 173°, Fig. 5a). This may be due to the existence of electrostatic interaction between MV^{2+} and SO_4^{2-}, leading to the SO_4^{2-} anion deviating from the optimal position to form hydrogen bonds. The 2 : 2 anion-to-ligand coordination of **4** is similar to that of **2**, but the counter-cations are bound in a different way. A 32.2°

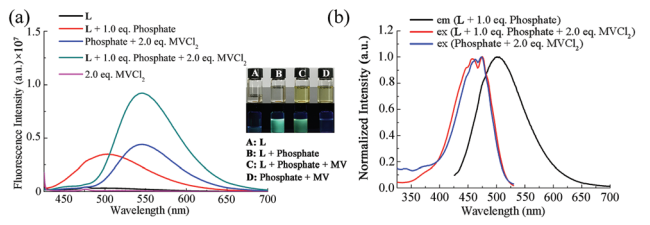

Fig. 3 (a) Fluorescence spectra (λ_{ex} = 415 nm) of L (1.0×10^{-4} M in DMSO), L with 1.0 equiv. of phosphate anions, L with 1.0 equiv. of phosphate anions and 2.0 equiv. of $MVCl_2$, and phosphate anions (1.0×10^{-4} M in DMSO) with 2.0 equiv. of $MVCl_2$; (b) emission spectra of L with 1.0 equiv. of phosphate anions (λ_{ex} = 415 nm) and excitation spectra of L with 1.0 equiv. of phosphate anions and 2.0 equiv. of $MVCl_2$ (λ_{em} = 547 nm) and only phosphate anions (1.0×10^{-4} M in DMSO) with 2.0 equiv. of $MVCl_2$ (λ_{em} = 547 nm).

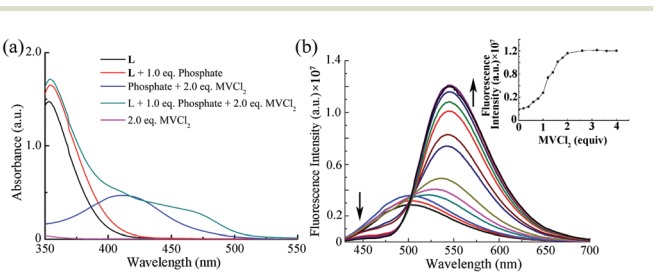

Fig. 4 (a) Absorption spectra of L upon the addition of 1.0 equiv. of phosphate anions and both 1.0 equiv. of phosphate anions and 2.0 equiv. of $MVCl_2$, and only phosphate anions and 2.0 equiv. of $MVCl_2$. (1.0×10^{-4} M in DMSO); (b) fluorescence titrations of phosphate complex **1** (1.0×10^{-4} M in DMSO) upon the addition of 0–4.0 equiv. of $MVCl_2$. Inset: The increase of the fluorescence intensity at λ = 544 nm.

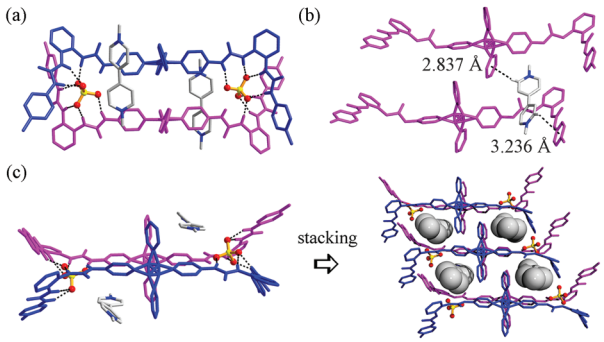

Fig. 5 Crystal structure of $[(MV)LSO_4]_2$ (**4**). (a) View along the *a* axis with the hydrogen bonds between SO_4^{2-} and ligands; (b) CH···π interactions between the MV^{2+} guest and **L** of the SO_4^{2-} complex (the anion and part symmetric **L** and MV^{2+} were omitted for clarity); (c) the side view and stacking mode of complex **4** (part non-acidic hydrogen atoms and solvents were omitted for clarity).

torsion angle between two pyridine rings of MV^{2+} can be observed instead of a coplanar configuration, which should be due to the formation of the CH···π interaction between MV^{2+} and the dangling phenyl rings of TPE (2.837 Å of C65–H65···phenyl, Fig. 5b), as well as the CH···π interaction between another MV^{2+} and the terminal aryls of **L** (3.236 Å of C62–H62···phenyl, Fig. 5b). It can be seen from the packing mode of the crystal structure that two MV^{2+} cations insert between two $[(SO_4)_2(\mathbf{L})_2]^{4-}$ dimers and are close to the two dangling phenyl rings of TPE (Fig. 5c).

Moreover, the ^1H NMR spectra of complex **4** and guest $MVCl_2$ show that MV^{2+} in **4** exhibits a slight upfield shift, indicating the shielding effect caused by the interaction with the sulfate complex (pyridine: $\Delta\delta$ = −0.16 and −0.15 ppm, $-CH_3$: $\Delta\delta$ = −0.11 ppm, Fig. 6a). The ESI-MS spectrum of complex **4** (Fig. 6b) further supports the coexistence of $[(SO_4)_2(\mathbf{L})_2]^{4-}$ and MV^{2+} by overlapping peaks of $[\mathbf{L}_4(SO_4)_4(MV)_2]^{4-}$ (obsd 1086.21 *vs.* calcd 1086.14), $[\mathbf{L}_2(SO_4)_2(MV)_1]^{2-}$ (obsd 1085.95 *vs.* calcd 1085.89), and $[\mathbf{L}_4(SO_4)_4(TBA)_2(MV)_1]^{4-}$ (obsd 1160.83 *vs.* calcd 1160.75).

By comparing the fluorescence and UV-vis spectra of **1** and **2** upon the addition of MV^{2+}, similar changes can be observed (Fig. S32b and S33†). So it is reasonable to speculate the binding mode between complex **1** and MV^{2+} based on complex **4**, which means that multiple CH···π and electrostatic interactions between MV^{2+} and the phosphate complex should also

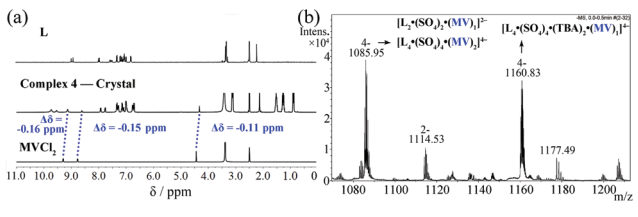

Fig. 6 (a) ^1H NMR spectra (400 MHz, 298 K, $[D_6]$DMSO) of L, complex **4** and guest $MVCl_2$; (b) high-resolution ESI mass spectra of complex **4**.

exist in complex **3**. PM6 calculations of **3** showed the rationality of this structure (Fig. S35†).

We have designed a bis–bis(urea) ligand (**L**) by incorporating the tetraphenylethene (TPE) fluorophore. The weakly emissive **L** in a dilute solution displays a large fluorescence enhancement with the addition of phosphate or sulfate anions, which is due to the restriction of TPE cores through anion coordination. More interestingly, the fluorescence of the anion complex shows a second enhancement with an accompanying red shift upon adding methyl viologen dichloride ($MVCl_2$). Crystal structures, fluorescence, UV-vis spectra, and NMR and ESI-MS results demonstrate the stable existence of the phosphate/sulfate complexes containing MV^{2+} and multiple interactions between them. The above multi-level assembly processes provide a supramolecular strategy for stepwise enhancement of fluorescence.

Conflicts of interest

There are no conflicts to declare.

Acknowledgements

We are grateful for the financial support from the National Natural Science Foundation of China (21772154).

Notes and references

1 (*a*) G. Yu, G. Tang and F. Huang, *J. Mater. Chem. C*, 2014, **2**, 6609–6617; (*b*) G. Yu, M. Zhang, M. L. Saha, Z. Mao, J. Chen, Y. Yao, Z. Zhou, Y. Liu, C. Gao, F. Huang, X. Chen and P. J. Stang, *J. Am. Chem. Soc.*, 2017, **139**, 15940–15949; (*c*) J. Li, K. Liu, H. Chen, R. Li, M. Drechsler, F. Bai, J. Huang, B. Z. Tang and Y. Yan, *ACS Appl. Mater. Interfaces*, 2017, **9**, 21706–21714.

2 (*a*) G. v. Bünau, *J. B. Birks: Photophysics of Aromatic Molecules*, Wiley-Interscience, London, 1970; (*b*) S. W. Thomas, G. D. Joly and T. M. Swager, *Chem. Rev.*, 2007, **107**, 1339–1386.

3 (*a*) Y. Hong, J. W. Y. Lam and B. Z. Tang, *Chem. Soc. Rev.*, 2011, **40**, 5361–5388; (*b*) J. Luo, Z. Xie, J. W. Y. Lam, L. Cheng, H. Chen, C. Qiu, H. S. Kwok, X. Zhan, Y. Liu, D. Zhu and B. Z. Tang, *Chem. Commun.*, 2001, **37**, 1740–1741.

4 N. B. Shustova, B. D. McCarthy and M. Dincă, *J. Am. Chem. Soc.*, 2011, **133**, 20126–20129.

5 K. Dhara, Y. Hori, R. Baba and K. Kikuchi, *Chem. Commun.*, 2012, **48**, 11534–11536.

6 Y. Chen, W. Zhang, Y. Cai, R. T. K. Kwok, Y. Hu, J. W. Y. Lam, X. Gu, Z. He, Z. Zhao, X. Zheng, B. Chen, C. Gui and B. Z. Tang, *Chem. Sci.*, 2017, **8**, 2047–2055.

7 (*a*) Y. Li, Y. Dong, L. Cheng, C. Qin, H. Nian, H. Zhang, Y. Yu and L. Cao, *J. Am. Chem. Soc.*, 2019, **141**, 8412–8415; (*b*) L. Xu, Z. Wang, R. Wang, L. Wang, X. He, H. Jiang,

H. Tang, D. Cao and B. Z. Tang, *Angew. Chem., Int. Ed.*, 2020, **59**, 9908–9913.

8 M. Hu, H.-T. Feng, Y.-X. Yuan, Y.-S. Zheng and B. Z. Tang, *Coord. Chem. Rev.*, 2020, **416**, 213329.

9 (*a*) P. Wang, X. Miao, Y. Meng, Q. Wang, J. Wang, H. Duan, Y. Li, C. Li, J. Liu and L. Cao, *ACS Appl. Mater. Interfaces*, 2020, **12**, 22630–22639; (*b*) W. Shang, X. Zhu, T. Liang, C. Du, L. Hu, T. Li and M. Liu, *Angew. Chem., Int. Ed.*, 2020, **59**, 12811–12816.

10 (*a*) E. Jin, J. Li, K. Geng, Q. Jiang, H. Xu, Q. Xu and D. Jiang, *Nat. Commun.*, 2018, **9**, 4143; (*b*) Y. Lan, X. Han, M. Tong, H. Huang, Q. Yang, D. Liu, X. Zhao and C. Zhong, *Nat. Commun.*, 2018, **9**, 5274.

11 (*a*) S.-Q. Xu, X. Zhang, C.-B. Nie, Z.-F. Pang, X.-N. Xu and X. Zhao, *Chem. Commun.*, 2015, **51**, 16417–16420; (*b*) Y. Li, Y. Dong, X. Miao, Y. Ren, B. Zhang, P. Wang, Y. Yu, B. Li, L. Isaacs and L. Cao, *Angew. Chem., Int. Ed.*, 2018, **57**, 729–733.

12 Z. Zhang, Z. Zhao, Y. Hou, H. Wang, X. Li, G. He and M. Zhang, *Angew. Chem., Int. Ed.*, 2019, **58**, 8862–8866.

13 C. Zhang, Z. Wang, L. Tan, T.-L. Zhai, S. Wang, B. Tan, Y.-S. Zheng, X.-L. Yang and H.-B. Xu, *Angew. Chem., Int. Ed.*, 2015, **54**, 9244–9248.

14 J. Dong, X. Li, K. Zhang, Y. Di Yuan, Y. Wang, L. Zhai, G. Liu, D. Yuan, J. Jiang and D. Zhao, *J. Am. Chem. Soc.*, 2018, **140**, 4035–4046.

15 S.-N. Lei, H. Xiao, Y. Zeng, C.-H. Tung, L.-Z. Wu and H. Cong, *Angew. Chem., Int. Ed.*, 2020, **59**, 10059–10065.

16 (*a*) H. Duan, Y. Li, Q. Li, P. Wang, X. Liu, L. Cheng, Y. Yu and L. Cao, *Angew. Chem., Int. Ed.*, 2020, **59**, 10101–10110; (*b*) J.-B. Xiong, H.-T. Feng, J.-P. Sun, W.-Z. Xie, D. Yang, M. Liu and Y.-S. Zheng, *J. Am. Chem. Soc.*, 2016, **138**, 11469–11472; (*c*) H. Qu, Y. Wang, Z. Li, X. Wang, H. Fang, Z. Tian and X. Cao, *J. Am. Chem. Soc.*, 2017, **139**, 18142–18145.

17 (*a*) W. Wang, Y.-X. Wang and H.-B. Yang, *Chem. Soc. Rev.*, 2016, **45**, 2656–2693; (*b*) J. Zhao, D. Yang, X.-J. Yang and B. Wu, *Coord. Chem. Rev.*, 2019, **378**, 415–444.

18 (*a*) B. Li, B. Zheng, W. Zhang, D. Zhang, X.-J. Yang and B. Wu, *J. Am. Chem. Soc.*, 2020, **142**, 6304–6311; (*b*) J. Fu, B. Zheng, H. Zhang, Y. Zhao, D. Zhang, W. Zhang, X.-J. Yang and B. Wu, *Chem. Commun.*, 2020, **56**, 2475–2478.

19 (*a*) D. Yang, J. Zhao, L. Yu, X. Lin, W. Zhang, H. Ma, A. Gogoll, Z. Zhang, Y. Wang, X.-J. Yang and B. Wu, *J. Am. Chem. Soc.*, 2017, **139**, 5946–5951; (*b*) W. Zhang, D. Yang, J. Zhao, L. Hou, J. L. Sessler, X.-J. Yang and B. Wu, *J. Am. Chem. Soc.*, 2018, **140**, 5248–5256.

20 J. Zhao, D. Yang, Y. Zhao, X.-J. Yang, Y.-Y. Wang and B. Wu, *Angew. Chem., Int. Ed.*, 2014, **53**, 6632–6636.

21 (*a*) S. Li, C. Jia, B. Wu, Q. Luo, X. Huang, Z. Yang, Q.-S. Li and X.-J. Yang, *Angew. Chem., Int. Ed.*, 2011, **50**, 5721–5724; (*b*) X. Bai, C. Jia, Y. Zhao, D. Yang, S.-C. Wang, A. Li, Y.-T. Chan, Y.-Y. Wang, X.-J. Yang and B. Wu, *Angew. Chem., Int. Ed.*, 2018, **57**, 1851–1855.

22 X.-F. Duan, J. Zeng, J.-W. Lü and Z.-B. Zhang, *J. Org. Chem.*, 2006, **71**, 9873–9876.

23 B. Limburg, E. Bouwman and S. Bonnet, *J. Phys. Chem. B*, 2016, **120**, 6969–6975.

24 A. W. H. Mau, J. M. Overbeek, J. W. Loder and W. H. F. Sasse, *J. Chem. Soc., Faraday Trans. 2*, 1986, **82**, 869–876.